Available online at www.sciencedirect.com
ScienceDirect
Journal of Power Sources 174 (2007) 795–799
JOURNAL OF POWER SOURCES
www.elsevier.com/locate/jpowsour

Short communication

Investigation of positive electrodes after cycle testing of high-power Li-ion battery cells II An approach to the power fading mechanism using hard X-ray photoemission spectroscopy

M. Shikano [a,*], H. Kobayashi [a], S. Koike [a], H. Sakaebe [a], E. Ikenaga [b], K. Kobayashi [b], K. Tatsumi [a]

[a] *National Institute of Advanced Industrial Science and Technology (AIST), 1-8-31 Midorigaoka, Ikeda, Osaka 63-8577, Japan*
[b] *Japan Synchrotron Radiation Research Institute (JASRI), 1-1-1 Kouto, Sayo-cho, Sayo-gun, Hyogo 679-5198, Japan*

Available online 28 June 2007

Abstract

X-ray photoemission spectroscopic and high-resolution hard X-ray photoemission spectroscopic studies of positive electrodes in $LiNi_{0.73}Co_{0.17}Al_{0.10}O_2$ and hard carbon based batteries were carried out to elucidate the mechanism of battery degradation. Li_2CO_3, hydrocarbons, $ROCO_2Li$, polycarbonate-type compounds and LiF were observed on positive electrode surfaces and the amount of carbonates was found to have increased after cycle testing. Above 60 °C, signs of electrolyte decomposition were indicated. Near the surface of the positive electrodes, a Li-deficient cubic phase is present and grows with degradation. Capacity and power fade could be related to the amount of species on the surface and the thickness of the Li-deficient cubic phase near the surface.

Keywords: Li-ion battery; Positive electrode; Hard X-ray photoemission spectroscopy; X-ray photoemission spectroscopy

1. Introduction

High-power battery technology is essential for hybrid electric vehicles and fuel cell vehicles. Vehicles like these use various alternative energy sources and are an attractive means to reduce carbon dioxide emissions. In obtaining the required high wattage, the characteristics of interfaces between electrolyte and both electrodes are very important. This is particularly so in the case of positive electrode surfaces, because their role in the mechanism of power degradation in high-power Li-ion cells is a significant one [1].

Lithium nickel oxide ($LiNiO_2$) based materials are promising for use as positive electrodes for high-power Li-ion cells because of their high power-to-energy ratio [1–4]. To improve and commercialize electrodes made from these materials, it is very important to determine their surface characteristics as mentioned above. Zhuang et al. reported that the formation of lithium carbonate (Li_2CO_3) on the surface of $LiNi_{0.8}Co_{0.15}Al_{0.05}O_2$ adversely impacts cell capacity and power [5]. Rahman and Saito's results using infrared spectroscopy (IR) indicated that the amount of Li_2CO_3 on the positive electrode surface decreased with an increase in state of charge (SOC) [6]. Andersson et al.'s study of electrode surfaces using X-ray photoemission spectroscopy (PES) showed positive electrode laminate surfaces to contain a mixture of organic species including polycarbonate-type compounds and lithium fluoride (LiF), Li_xPF_y-type and $Li_xPF_yO_z$-type compounds, while negative electrode laminate surfaces contained lithium alkyl carbonates ($ROCO_2Li$) and Li_2CO_3 in addition to the positive electrode surface compounds [7]. Furthermore, using techniques, such as transmission electron microscopy and X-ray absorption spectroscopy, Abraham et al. found that a change in electrode surface structure accompanied oxygen loss related aging of Li-ion cells [8]. Taken together, these results do not provide a clear picture.

In this study, high-resolution hard X-ray photoemission spectroscopy (HX-PES) was used to evaluate positive electrode

* Corresponding author. Tel.: +81 72 751 7932; fax: +81 72 751 9609.
E-mail address: shikano.masahiro@aist.go.jp (M. Shikano).

0378-7753/$ – see front matter © 2007 Elsevier B.V. All rights reserved.
doi:10.1016/j.jpowsour.2007.06.138

surface characteristics because of its large probe depth d. By controlling the take-off angle θ of photoelectrons in HX-PES, depth profiles of surfaces can be observed without sputtering because d is proportional to $\cos\theta$, that is, the condition of the electrode surface is maintained during measurement. We report the relationship between variations of species on positive electrode surfaces and degradation of Li-ion batteries after battery tests.

2. Experimental

Cylindrical cells with a capacity of ca. 420 mAh were used in this study. The positive electrodes consisted of a mixture of $LiNi_{0.73}Co_{0.17}Al_{0.10}O_2$, acetylene black (AB), and polyvinylidene fluoride (PVDF) binder, and the negative electrode was comprised of nongraphitizable carbon (hard carbon) and PVDF binder. A 1 mol dm^{-3} of $LiPF_6$ in propylene carbonate and dimethyl carbonate (volume ratio 3:2) was used as electrolyte. Details of cell chemistry are described elsewhere [2]. Each cell was characterized using a modified version, as detailed elsewhere, of the cycle test procedure in the PNGV Battery Test Manual [2,9,10]. Changes in cell capacity and dc resistance were tested at prescribed cycles or periods. Positive electrodes collected from cells under SOC control before and after cycle testing were washed with dimethyl carbonate then dried under vacuum at room temperature for more than 10 h. Species on surfaces were characterized by PES (JEOL JPS-9010MX spectrometer using Mg Kα radiation) and HX-PES ($h\nu$ = 8.0 keV). HX-PES was performed at BL47XU in SPring-8 with the approval of the Japan Synchrotron Radiation Research Institute as a Nanotechnology Support Project of Japan's Ministry of Education, Culture, Sports, Science and Technology (Proposal No. 2005B0713).

3. Results and discussion

The positive electrode was found to have maintained its initial crystal structure during cycle testing [2]. However, the Li content of both electrodes at SOC = 0% and 100% changed from that in the cell initially with increasing capacity fade [2]. Therefore, imbalance of Li content between positive and negative electrode due to an apparent migration of Li to the negative electrode can be thought to cause capacity fade. In the case of power fade, we should consider the properties of the positive electrode surface.

3.1. Species on the positive electrode

C 1s, O 1s and F 1s core-level PES spectra of a positive electrode from a cell before cycle tests are shown in Fig. 1. The positive electrode is a mixture of $Li_xNi_{0.73}Co_{0.17}Al_{0.10}O_2$ (LMO), acetylene black (AB) and polyvinylidene fluoride (PVDF), as active material, conductive material and binder, respectively. C 1s spectra show six peaks at 284.3, 285.4, 286.5, 288.1, 290.0 and 290.4 eV. The strong peak at 284.3 eV should be AB. Peaks at 286.5 and 290.4 eV are assigned to C–H and C–F of PVDF, respectively [7,11–14]. The other peaks

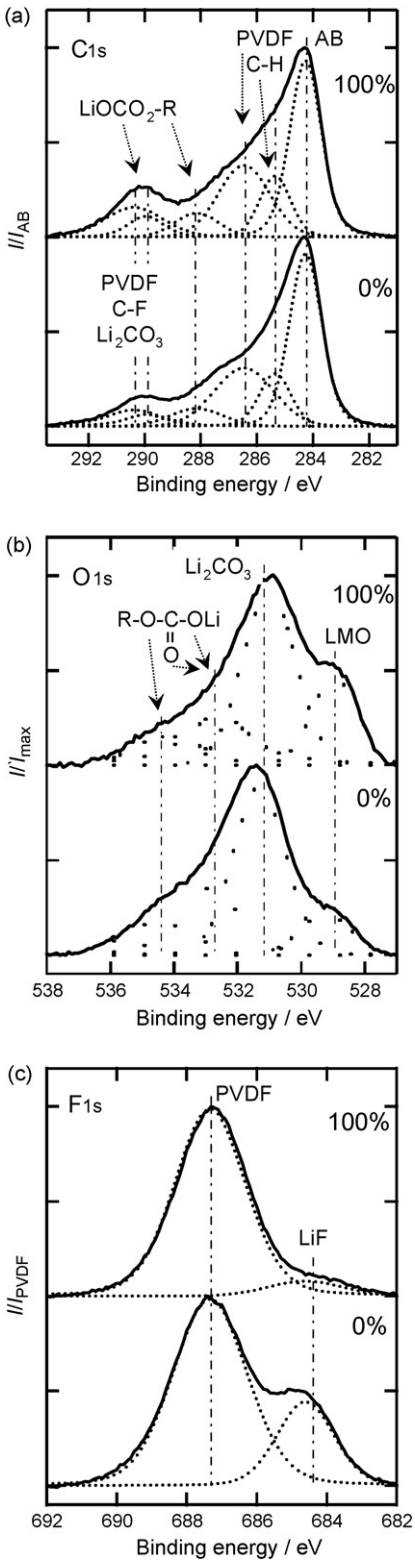

Fig. 1. PES spectra of a positive electrode from a cell before cycle tests: (a) C 1s, (b) O 1s and (c) F 1s core level. Lower and upper spectra correspond to SOC = 0% and 100%, respectively.

are judged to be Li_2CO_3 and organic species, such as hydrocarbons, $ROCO_2Li$ and polycarbonate-type compounds. The two peaks in the O 1s spectra at 529.3 and 531.3 eV correspond to LMO and Li_2CO_3, respectively [11,13,14]. Peaks

at 532.9 and 534.5 eV can be explained as $ROCO_2Li$ and polycarbonate-type compound [7,12–14]. F 1s spectra show two profiles of 687.3 eV (PVDF and/or $LiPF_6$) and 684.6 eV (LiF). After Ar sputtering, the weak P 1s spectrum disappeared, but the 687.3 eV peak remained. Therefore, the 687.3 eV peak can be assigned mainly to PVDF. Li_2CO_3, hydrocarbons, $ROCO_2Li$, polycarbonate-type compounds and LiF are present on the surface of positive electrodes of cells prior to testing. As shown in Fig. 1b, in the case of SOC = 100%, peak representing LMO at 529.3 eV is stronger than that in the case of SOC = 0%, that is, amounts of Li_2CO_3, $ROCO_2Li$ and polycarbonate-type compounds decrease with charging. This finding is in harmony with the results of a previous IR study [6].

Fig. 2 shows HX-PES of a positive electrode from a cell before and after cycle tests. After the tests at 40, 60 and 80 °C, relative capacities were 99.7%, 95.0% and 81.2%, and relative dc resistances were 1.1, 1.3 and 1.8, respectively; details of the tests are reported elsewhere [1,2]. SOC was kept at 0% to render the charge–discharge effect negligible. The C 1s peak of hydrocarbons is not significant (Fig. 2a) because d of HX-PES is around 20 nm and hydrocarbons are present only on the surface of the positive electrode. Fig. 2b shows O 1s HX-PES spectra. In the case of 40 °C, only Li_2CO_3 increases after the test. In the case of 80 °C, the amount of all carbonates, such as Li_2CO_3 and $ROCO_2Li$, and polycarbonate-type compounds is significantly larger than the initial cell. In the case of 60 °C, Li_2CO_3 significantly increases while $ROCO_2Li$ and polycarbonate-type compounds increase slightly. One can thus say that electrolyte decomposition during testing occurred above 60 °C. An increase in Li_2CO_3 should relate to both power and capacity fades, because the source of Li should be LMO and the resistivity of Li_2CO_3 is very high. Moreover, the electrolyte decomposition induces power fade because of the high resistivity of the organic products.

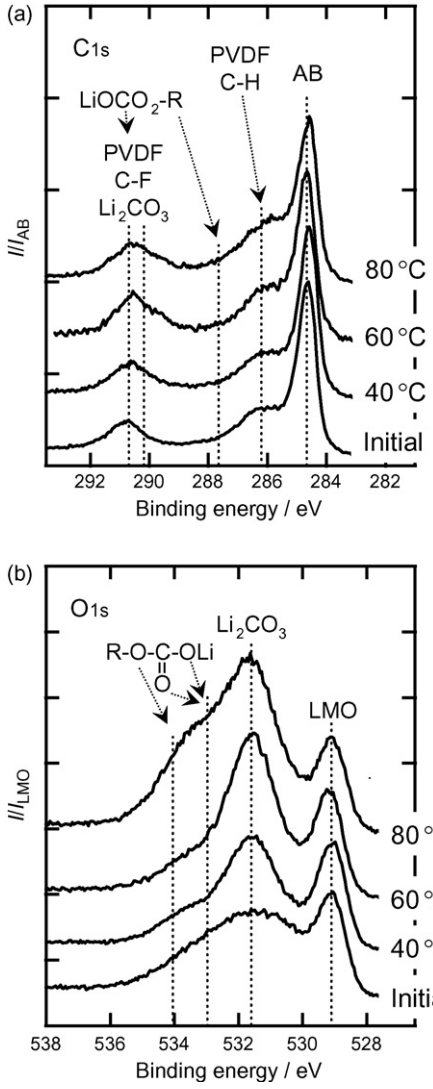

Fig. 2. HX-PES ($\theta = 10°$) spectra of a positive electrode from a cell before and after cycle tests at 40, 60 and 80 °C: (a) C 1s and (b) O 1s core level. SOC was kept at 0%.

3.2. Degradation of the surface

Almost all Ni $2p_{3/2}$ core-level PES spectra after Ar sputtering are very similar to the NiO spectrum [15], which means that the surface of LMO is easily reduced under vacuum and changes to a NiO-like structure. Without sputtering, Ni $2p_{3/2}$ spectra are decomposed into 854.5, 856.0, 860.6 and 863.0 eV peaks (Fig. 3a). The shapes of Ni $2p_{3/2}$ spectra are different from those of NiO [15] and $LiNiO_2$ [16], while the binding energies of the peaks are very close to those of NiO [15]. The 856.0 eV peak should contain a higher valence state of Ni ions, because it is stronger in the case of SOC = 100% than in the case of SOC = 0%. Ni 2p profiles are thus recognized as containing NiO-like components (854.5 and 856.0 eV) and a Ni^{3+} component (856.0 eV) [8]. Abraham et al. suggested the thickness of a NiO-like film on the electrode surface to be around 2–4 nm [8]. The probe depth of PES, which is estimated to be around 2–3 nm, is consistent with Abraham et al.'s film thickness. On the other hand, the probe depth of HX-PES is estimated to be 10 times as large as that of PES; therefore, HX-PES spectra contain information on bulk structure as well as surface structure. Ni $2p_{3/2}$ HX-PES spectra are also decomposed into four peaks: 855.2, 855.8, 861.0 and 863.0 eV (Fig. 3b). The binding energies of two satellites of a shake-up structure, 861.0 and 863.0 eV, are similar to those in the PES spectra but very weak. This is especially so in the case of SOC = 100%, where these two satellites seem to have disappeared. In the HX-PES spectra, the component due to the NiO-like structure is minor, because its thickness is much smaller than the HX-PES probe depth. If the NiO-like structure is the same as $Ni^{2+}O$, NiO profiles should appear independent of SOC. Thus, the NiO-like structure can be considered as a Li-deficient cubic phase, namely $Li_{0.5-x}(Ni,Co,Al)_{0.5}O$. A model of the surface of the positive electrode can thus be drawn as in Fig. 4. Continuous change in phase is present from the surface to the bulk of positive electrode, with carbonates and LiF on the surface. Full widths at half maximum (FWHM) of 855.2 and 855.8 eV peaks are 2.3 and 3.3 eV in the case of SOC = 0% and 2.7 and 1.6 eV in the case of SOC = 100%, respectively. The difference between FWHM of the 855.2 eV peak is slight, while

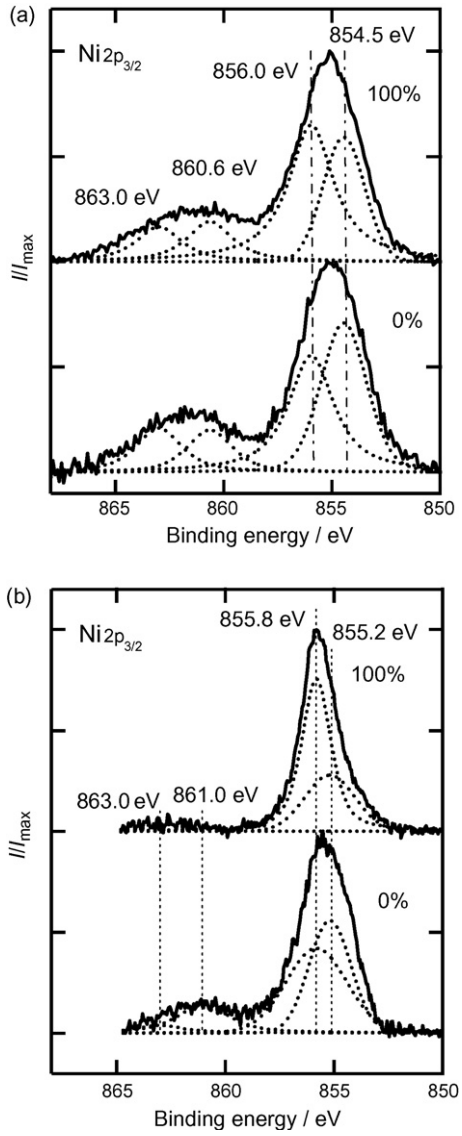

Fig. 3. Ni $2p_{3/2}$ core-level (a) PES and (b) HX-PES ($\theta = 10^\circ$) spectra of a positive electrode from a cell before cycle tests. Lower and upper spectra correspond to SOC = 0% and 100%, respectively.

the difference between FWHM of the 855.8 eV peak is significant. In the case of SOC = 0%, Li content x of LMO is higher than that in the case of SOC = 100%, that is, the compositional slope between the Li-deficient cubic phase and LMO is steeper in the case of SOC = 0%. Therefore, in the case of SOC = 0%, variation in the Ni-ion states, or FWHM, should be greater. Near

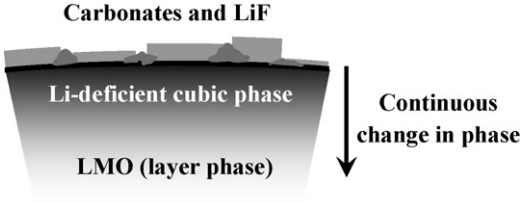

Fig. 4. Schematic representation of the surface of a positive electrode from a cell before cycle tests.

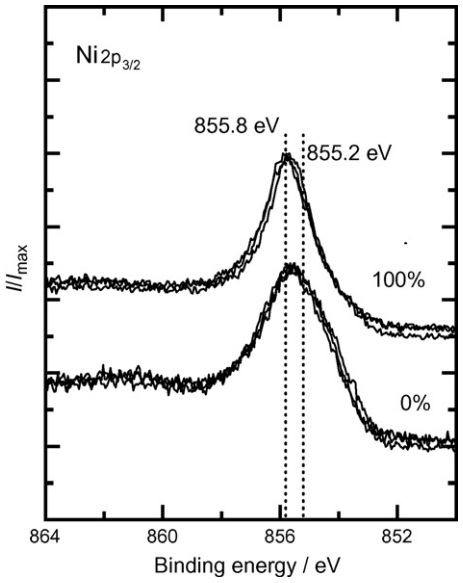

Fig. 5. Ni $2p_{3/2}$ core-level HX-PES ($\theta = 10^\circ$) spectra of a positive electrode from a cell before and after cycle testing at 40 and 60 °C. SOC was kept at 0% and 100%.

the surface, on the other hand, Ni ions in the Li-deficient cubic phase can remain in the same environment and the change of FWHM should thus be independent of SOC. Through comparison of Fig. 3a and b, 855.2 and 855.8 eV peaks are assigned as overlap of $Ni^{2+/3+}$ in the Li-deficient cubic phase and $Ni^{3+/4+}$ in LMO and in the intermediate state of LMO and the Li-deficient cubic phase. Therefore, in the case of SOC = 100%, the 855.8 eV peak is larger than that in SOC = 0%. Two peaks in the Ni $2p_{3/2}$ PES spectrum are recognized as components of the Li-deficient cubic phase near the surface.

Fig. 5 shows Ni $2p_{3/2}$ core-level HX-PES spectra of a positive electrode used in a cell before and after cycle tests. All profiles are similar to each other, independent of the test conditions, and obey SOC. In the bulk of the electrode, results of X-ray adsorption near edge structure spectroscopy have shown that the valence state of Ni ions is not disturbed by cycle testing [2]. Therefore, HX-PES spectra are close to the bulk information. On the other hand, in the case of $\theta = 60^\circ$, a difference is seen in Ni $2p_{3/2}$ core-level HX-PES spectra of the cell before and after testing (Fig. 6). The HX-PES probe depth is reduced to half of $\theta = 10^\circ$ because of $\cos 10^\circ \approx 2\cos 60^\circ$. The main peaks of Ni $2p_{3/2}$ core-level HX-PES spectra are decomposed into 855.0 and 856.0 eV. The area ratio of the 855.0 eV peak in the main profile of Ni $2p_{3/2}$ spectra is 31% before and 22% after the cycle test at 60 °C, that is, the valence state of Ni ions near the surface increases with cycle testing. After the cycle tests, the amount of Li defects increases because of the capacity fade. On the other hand, the valence state of Ni ions in the bulk remains in the same condition after testing. Therefore, the Li defect develops mainly near the surface. We can say that the cycle test grew the structure, the Li-deficient cubic phase, near the surface (Fig. 7). Li conductivity of the Li-deficient cubic phase should be lower than that of LMO because Li ions, transition metal ions and vacancies are mixed randomly at the same site in the case of the

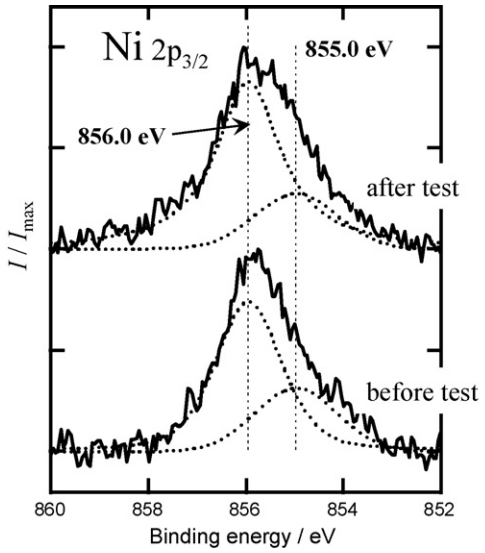

Fig. 6. Ni $2p_{3/2}$ core-level HX-PES ($\theta = 60°$) spectra for a positive electrode from a cell before and after cycle testing at 60 °C. SOC was kept at 100%.

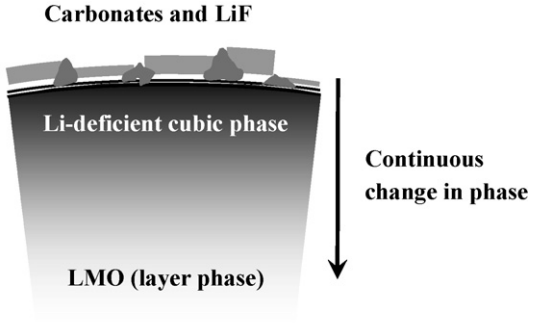

Fig. 7. Schematic representation of a positive electrode surface after cycle testing. The amount of species on the surface and the thickness of the Li-deficient cubic phase near the surface increased after testing.

cubic phase. The thickness of the structure therefore should be related to the power fade of the cells.

4. Conclusion

PES and HX-PES studies were performed on positive electrodes used in high-power batteries. Li_2CO_3, hydrocarbons, $ROCO_2Li$, polycarbonate-type compounds and LiF were observed on positive electrode surfaces. The amount of carbonates increased after cycle testing. Signs of electrolyte decomposition were indicated at temperatures above 60 °C. A Li-deficient cubic phase exists near the surface of the positive electrode and grows with degradation. Capacity and power fade could be related to the amount of species on the surface and to the thickness of the Li-deficient cubic phase near the surface.

Acknowledgements

This work was financially supported by the New Energy and Industrial Technology Development Organization and the Ministry of Economy, Trade and Industry in Japan as part of the Development of Lithium Battery Technology for Use by Fuel Cell Vehicles project, FY2002–FY2006. The authors would like to thank Mr. Ozaki of Matsushita Battery Industrial Co. Ltd., for supplying the battery cells used in this research and Mr. Kihira of Central Research Institute of Electric Power Industry for conducting the cycle tests. The authors would also like to express their gratitude for assistance received in discussions with Mr. Yoshiyasu Saito of AIST.

References

[1] N. Kihira, N. Terada, Proceedings of 22nd International Battery Hybrid and Fuel Cell Electric Vehicle Symposium & Exposition, Yokohama, 2006.
[2] H. Kobayashi, M. Shikano, S. Koike, H. Sakaebe, K. Tatsumi, J. Power Sources 174 (2007) 380.
[3] K. Amine, J. Liu, ITE Lett. 1 (2000) 59–63.
[4] K. Amine, C.H. Chen, J. Liu, M. Hammond, A. Jansen, D. Dees, I. Bloom, D. Vissers, G. Henriksen, J. Power Sources 97/98 (2001) 684–687.
[5] G.V. Zhuang, G. Chen, J. Shim, X. Song, P.N. Ross, T.J. Richardson, J. Power Sources 134 (2004) 293–297.
[6] Md. K. Rahman, Y. Saito, 208th ECS Meeting, abstract #198, 2005; Md. K. Rahman, Y. Saito, J. Power Sources 174 (2007) 889.
[7] A.M. Andersson, D.P. Abraham, R. Haasch, S. MacLaren, J. Liu, K. Amine, J. Electrochem. Soc. 149 (2002) A1358–A1369.
[8] D.P. Abraham, R.D. Twesten, M. Balasubramanian, J. Kropf, D. Fischer, J. McBreen, I. Petrov, K. Amine, J. Electrochem. Soc. 150 (2003) A1450–A1456.
[9] PNGV Battery Test Manual, Rev. 3, DOE/ID-10597, 2001.
[10] N. Kihira, Abstracts of the 46th Battery Symposium in Japan, 2005, pp. 566–567; N. Kihira, Y. Mita, E. Takei, Y. Kobayashi, H. Miyashiro, K. Kumai, N. Terada, T. Iwahori, 206th ECS Meeting, abstract #385, 2004.
[11] C.D. Wagner, A.V. Naumkin, A. Kraut-Vass, J.W. Allison, C.J. Powell, J.R. Rumble Jr., NIST X-ray Photoelectron Spectroscopy Database, NIST Standard Reference Database 20, Version 3.4, 2007.
[12] D. Bar-Tow, E. Peled, L. Burstein, J. Electrochem. Soc. 146 (1999) 824–832.
[13] A.M. Andersson, A. Henningson, H. Siegbahn, U. Jansson, K. Edström, J. Power Sources 119–121 (2003) 522–527.
[14] R. Dedryvère, L. Gireaud, S. Grugeon, S. Laruelle, J.-M. Tarascon, D. Gonbeau, J. Phys. Chem. B 109 (2005) 15868–15875.
[15] A.N. Mansour, Surf. Sci. Spectra 3 (1996) 231–238.
[16] A.N. Mansour, Surf. Sci. Spectra 3 (1996) 279–286.